

Study of surface damage in silicon by irradiation with focused rubidium ions using a cold-atom ion source

Citation for published version (APA):

Xu, S., Li, Y., Verheijen, M. A., Kieft, E. R., & Vredenburg, E. J. D. (2023). Study of surface damage in silicon by irradiation with focused rubidium ions using a cold-atom ion source. *Journal of Vacuum Science and Technology B*, 41(4), Article 042804. <https://doi.org/10.1116/6.0002643>

Document license:
CC BY

DOI:
[10.1116/6.0002643](https://doi.org/10.1116/6.0002643)

Document status and date:
Published: 01/07/2023

Document Version:
Publisher's PDF, also known as Version of Record (includes final page, issue and volume numbers)

Please check the document version of this publication:

- A submitted manuscript is the version of the article upon submission and before peer-review. There can be important differences between the submitted version and the official published version of record. People interested in the research are advised to contact the author for the final version of the publication, or visit the DOI to the publisher's website.
- The final author version and the galley proof are versions of the publication after peer review.
- The final published version features the final layout of the paper including the volume, issue and page numbers.

[Link to publication](#)

General rights

Copyright and moral rights for the publications made accessible in the public portal are retained by the authors and/or other copyright owners and it is a condition of accessing publications that users recognise and abide by the legal requirements associated with these rights.

- Users may download and print one copy of any publication from the public portal for the purpose of private study or research.
- You may not further distribute the material or use it for any profit-making activity or commercial gain
- You may freely distribute the URL identifying the publication in the public portal.

If the publication is distributed under the terms of Article 25fa of the Dutch Copyright Act, indicated by the "Taverne" license above, please follow below link for the End User Agreement:

www.tue.nl/taverne

Take down policy







If you believe that this document breaches copyright please contact us at:

openaccess@tue.nl

providing details and we will investigate your claim.

RESEARCH ARTICLE | JUNE 21 2023

Study of surface damage in silicon by irradiation with focused rubidium ions using a cold-atom ion source

S. Xu ; Y. Li ; M. A. Verheijen ; E. R. Kieft ; E. J. D. Vredenburg  



Journal of Vacuum Science & Technology B 41, 042804 (2023)

<https://doi.org/10.1116/6.0002643>



CrossMark

28 June 2023 08:50:39



Instruments for Advanced Science

- Knowledge
- Experience
- Expertise

Click to view our product catalogue

Contact Hiden Analytical for further details:
www.HidenAnalytical.com
info@hiden.co.uk



Gas Analysis

- dynamic measurement of reaction gas streams
- catalysis and thermal analysis
- molecular beam studies
- dissolved species probes
- fermentation, environmental and ecological studies



Surface Science

- UHV-TPD
- SIMS
- end point detection in ion beam etch
- elemental imaging - surface mapping



Plasma Diagnostics

- plasma source characterization
- etch and deposition process reaction kinetic studies
- analysis of neutral and radical species



Vacuum Analysis

- partial pressure measurement and control of process gases
- reactive sputter process control
- vacuum diagnostics
- vacuum coating process monitoring

Study of surface damage in silicon by irradiation with focused rubidium ions using a cold-atom ion source

Cite as: J. Vac. Sci. Technol. B 41, 042804 (2023); doi: 10.1116/6.0002643

Submitted: 6 March 2023 · Accepted: 30 May 2023 ·

Published Online: 21 June 2023



S. Xu,¹ Y. Li,¹ M. A. Verheijen,^{1,a)} E. R. Kieft,² and E. J. D. Vredenburg^{1,b)}

AFFILIATIONS

¹Department of Applied Physics, Eindhoven University of Technology, P.O. Box 513, Eindhoven 5600 MB, The Netherlands

²Thermo Fisher Scientific, Achtseweg Noord 5, Eindhoven 5651 GG, The Netherlands

^{a)}Also at: Eurofins Materials Science, High Tech Campus 11, Eindhoven 5656AE, The Netherlands

^{b)}Author to whom correspondence should be addressed: e.j.d.vredenburg@tue.nl

ABSTRACT

Cold-atom ion sources have been developed and commercialized as alternative sources for focused ion beams (FIBs). So far, applications and related research have not been widely reported. In this paper, a prototype rubidium FIB is used to study the irradiation damage of 8.5 keV beam energy Rb⁺ ions on silicon to examine the suitability of rubidium for nanomachining applications. Transmission electron microscopy combined with energy dispersive x-ray spectroscopy is applied to silicon samples irradiated by different doses of rubidium ions. The experimental results show a duplex damage layer consisting of an outer layer of oxidation without Rb and an inner layer containing Rb mostly at the interface to the underlying Si substrate. The steady-state damage layer is measured to be 23.2(±0.3) nm thick with a rubidium staining level of 7(±1) atomic percentage.

© 2023 Author(s). All article content, except where otherwise noted, is licensed under a Creative Commons Attribution (CC BY) license (<http://creativecommons.org/licenses/by/4.0/>). <https://doi.org/10.1116/6.0002643>

I. INTRODUCTION

Focused ion beam (FIB) techniques are widely applied in various research fields for imaging, nanomachining, and surface modification.^{1–3} Ion milling is one of the common uses in the semiconductor industry, such as for specific layer removal, cross sectioning, and transmission electron microscopy (TEM) sample preparation.⁴ However, during the FIB treatment, structural changes occur after repeated ion beam scanning, including defect production,⁵ amorphization,⁶ and ion mixing of materials,⁷ leading to device failure or degradation. Therefore, studies of damage effects are a necessary part of assessing the suitability of novel FIB instruments for applications.

Studies on ion damage using commercially available FIB instruments have been widely reported. The Ga FIB has been widely used and is popular for nanomachining applications. Previous study shows that Ga⁺ irradiation at 30 keV beam energy under normal incidence (0°) can lead to an amorphous layer with a thickness exceeding 50 nm with a Ga staining level of 20 at. %⁸

The formation of a Ga concentration layer near the sample surface is also reported if the ion dose is higher than 1.5×10^{17} ions/cm². For light ions, the helium gas field ionization ion source is commonly used,⁹ e.g., to generate nanostructures in the nanofilm¹⁰ or two-dimensional materials.¹¹ In bulk materials, He⁺ irradiation usually causes subsurface implantation and damage, such as nanobubbles in Si substrates.¹² This mainly results from the low sputter yield¹³ and high diffusivity¹⁴ of He⁺ in silicon.

Cold-atom ion sources (CAISs) are a relatively new development that can offer diverse ion species as well as high brightness and low energy spread,¹⁵ which can potentially reduce ion damage by allowing operation at low beam energy with good resolution. One novel FIB using a Cs⁺ CAIS was studied in detail¹⁶ and is now commercialized.¹⁷ However, experimental studies of ion-induced damage by cold-atom FIBs are still rare. Using a conventional Cs source, it was shown that normal incidence Cs⁺ irradiation at beam energy of 14.5 keV on Si leads to a 25 nm thick amorphous layer with a staining level of around 10 at. %¹⁸

28 June 2023 08:50:39

Employing $\text{Rb}^{+19,20}$ provides an alternative to the Cs^{+} CAIS and was also shown to enable low energy spread when operated at beam energies under 10 keV.²¹ Previous work also demonstrated that Rb^{+} ions have good sputtering ability for various substrates²² at this beam energy and allow ion beam induced deposition of Pt with a conventional precursor.²³ In this paper, we consider the irradiation damage caused by Rb^{+} ion milling of Si substrates as a further test of suitability. Here, silicon is chosen to be the substrate due to its broad use in semiconductor devices. We limit ourselves to irradiation at normal incidence, which is more appropriate for targeting the circuit edit application rather than lamella preparation, which requires glancing angles. To characterize the subsurface damage, irradiated regions were cross sectioned and thinned to produce lamellae. These lamellae were then analyzed by high-resolution TEM combined with energy dispersive x-ray spectroscopy (EDS) to obtain the top-down structural evolution. This work presents new insight into the Rb^{+} irradiation damage, especially microstructural changes in the amorphous layer.

II. EXPERIMENT

The Rb^{+} irradiation damage tests were performed in a prototype Rb CAIS-FIB instrument, which is illustrated in Fig. 1(a). In the CAIS-FIB system, the collimated Rb atom beams are first laser-cooled and compressed in a magneto-optical compressor, then further cooled down by a postcooling process, and finally,

photoionized to the Rb^{+} ion beams by two-step photoionization. The basic concept of CAIS can be found in McClelland *et al.*,¹⁵ and the details of the Rb CAIS-FIB are described in Refs. 19, 20, and 24–26. Since a CW laser is used for photoionization and Rb has a single valence electron, the formation of doubly-charged ions is unlikely. The formation of molecular ions furthermore seems incompatible with the low density of the atomic beam. Therefore, the Rb ion beam is expected to consist almost entirely of singly-charged ions, even with isotopic purity. A fraction of the Rb atomic beam will not be ionized and reach the sample area with a kinetic energy of order 100 meV, which is too low to contribute to sputtering. We note, however, that experiments to validate these expectations have not been reported. Due to the gaussian-like transverse profile of atomic and photoionization beams, the ion beam from a CAIS does show a halo not unlike that observed with Ga ion beams.

The experiments were performed as the following steps: (1) the Si substrates were irradiated by Rb^{+} ion beams in a prototype Rb CAIS-FIB instrument at a normal incidence, as shown in Fig. 1(b); (2) use a Dual-beam FIB system to prepare TEM lamellae [see Fig. 1(c)]; and (3) the lamellae were characterized in the TEM instrument to observe the damage layer. In this work, a series of $12 \times 2 \mu\text{m}^2$ rectangles were irradiated under Rb^{+} ion beams at a beam current of 4 pA and a beam energy of 8.5 keV, which is currently the highest beam energy permitted by the design of the CAIS. The stability of the beam current during milling was 0.2 pA, which, in principle, could be improved by adjusting the

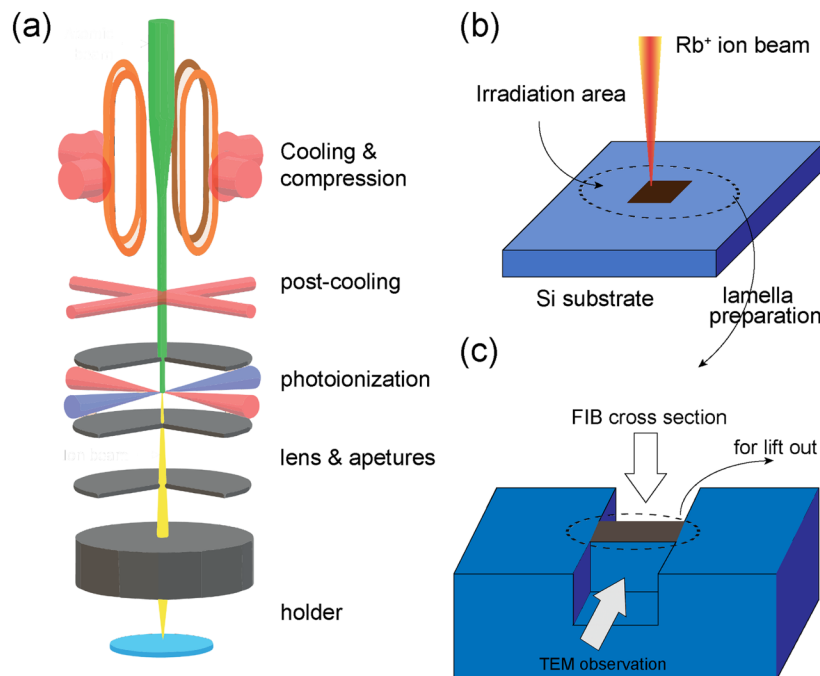


FIG. 1. (a) Brief illustration of the Rb CAIS-FIB system; (b) Rb^{+} ion beams irradiation on the Si substrate; (c) cross-section process for lamella preparation for ion damage study.

28 June 2023 08:50:39

photoionization laser power dependent on beam current (e.g., observation of sample current) in a feedback loop. Detailed experimental measurements of the current produced by the Rb CAIS can be found in Ref. 26, where the maximum current achieved was 600 pA. For each pattern, the dwell time is 1 μ s and the overlap is 50%. The spot size of the Rb⁺ ion beam under these conditions was around 160 nm, and the chamber vacuum is lower than 2×10^{-6} mbar during irradiation. Substantially smaller spot sizes down to a few nm should be possible²⁴ under optimum conditions but require operation in a different regime, which has not been explored yet.

The (100) silicon substrates were obtained commercially from Ted Pella Inc with ultrahigh purity. The silicon wafer was cleaned using ethanol and dried afterward before being mounted in the FIB chamber. After irradiation, the silicon substrates were transported to a Dual-beam FIB for the lamella preparation.

To enable TEM characterization of the irradiated silicon substrate, the standard FIB cross-section lift-out method²⁷ in a FEI Nova Nanolab Dual-beam FIB system was used. Before cross sectioning, the irradiated regions were covered by 300 nm of

electron-induced Pt deposition and then by 1 μ m of ion-induced Pt deposition as support and protection. The FIB lamellae were cut out using a Ga⁺ ion beam with a beam energy of 30 keV and a beam current of around 2 nA. A tungsten needle was used for lifting out the lamella and transporting it onto a half Cu grid. Subsequently, the lamellae were processed to electron transparency with a 30 keV Ga⁺ ion beam at a beam current of 93 pA and a milling time of 3 min per side. In the final polishing step, a beam shower was made onto each side of the lamellae under 5 keV and, finally, a 2 keV Ga⁺ ion beam to reduce the Ga⁺ ion staining and sidewall amorphization.

The lamella samples were characterized in an FEI Titan Cubed 60-300 operated at 300 kV and a JEOL ARM 200F working at 200 kV. Images were acquired both in high-resolution transmission electron microscopy (HRTEM) mode and in the high-angle annular dark field (HAADF) scanning transmission electron microscopy (STEM) mode. EDS was performed using the Super-X G2 (Titan) and Centurio SDD (ARM 200F) detectors in the STEM mode. The expected EDS measurement accuracy is approximately 1% and 2% for heavy and light elements, respectively. Distance

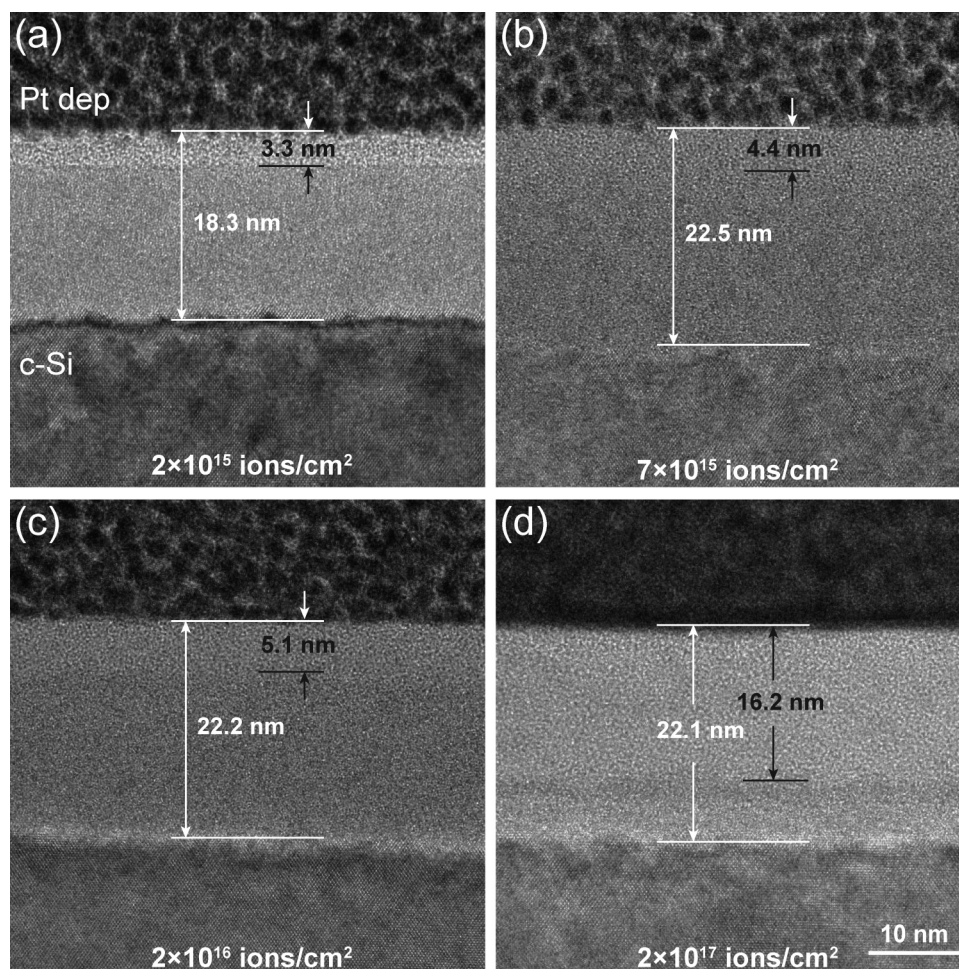


FIG. 2. HRTEM images of Si substrates irradiated at normal incidence under various Rb⁺ ion doses: (a) 2×10^{15} ions/cm² with 18.3(±0.3) nm damage layer, (b) 7×10^{15} ions/cm² with 22.5(±0.4) nm damage layer, (c) 2×10^{16} ions/cm² with 22.2(±0.2) nm damage layer, (d) 2×10^{17} ions/cm² with 22.1(±0.3) nm damage layer.

28 June 2023 08:50:39

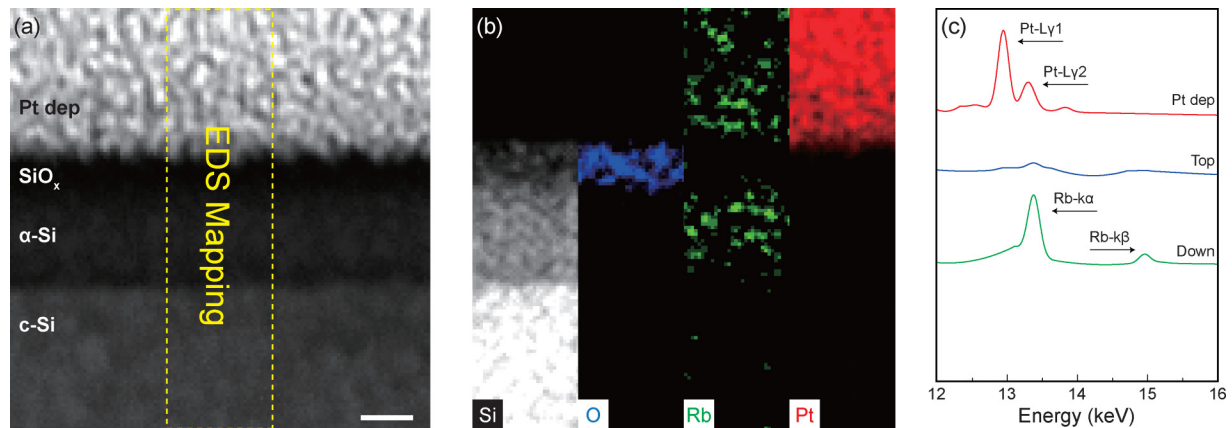


FIG. 3. (a) HAADF-STEM image of a cross-section Si sample irradiated with a 2×10^{16} ions/cm² ion dose. The indicated (yellow) box inset shows the EDS mapping area. (b) EDS mapping results of the selected area in (a) for four elements, from left to right representing Si (white), O (blue), Rb (green), and Pt (red). (c) The energy spectra for the four layers shown in (a) with the range in 12–16 keV. Scale bar, 10 nm.

measurements on substrates have an estimated statistical uncertainty of typically 0.3 nm as determined by repeated measurements at different positions.

III. RESULTS AND DISCUSSION

The Rb⁺ ion damage study starts with a series of irradiations on Si (100) substrates for various ion doses. Figure 2 shows the HRTEM images of the irradiated Si samples under four different ion doses. At the lowest dose of 2×10^{15} ions/cm², an amorphous layer of $18.3(\pm 0.3)$ nm is visible. When the dose is increased to 7×10^{15} ions/cm², the thickness is increased to $22.5(\pm 0.4)$ nm. For even higher ion dose irradiations of 2×10^{16} and 2×10^{17} ions/cm², the damage layer is measured as $22.2(\pm 0.2)$ and $22.1(\pm 0.3)$ nm, as shown in Figs. 2(c) and 2(d), respectively. These results show a constant amorphization depth of the silicon substrate by Rb⁺ ions as a function of dose for all but the lowest dose. At the lowest dose, the damage layer is shown to be around 18.3 nm, as shown in Fig. 2(a), which is different from the amorphization process that shows a generally increasing thickness in the amorphous layer as described by Drezner *et al.*¹⁸ Apart from that, another observation is the stratification in the damage layer. The topmost part of each damaged layer shows increased brightness in the HRTEM images. The thickness of the top layer starts from $3.3(\pm 0.1)$ nm at the dose of 2×10^{15} ions/cm², generally increases to $4.4(\pm 0.1)$ nm and $5.1(\pm 0.1)$ nm, and reaches $16.2(\pm 0.2)$ nm at the highest dose of 2×10^{17} ions/cm². It is also noticed that the brighter layer is visible in Figs. 2(a) and 2(d), but not clear to be seen in (b) and (c). Corresponding TEM images at lower magnification are shown additionally in the Supplementary material,³⁰ where the amorphous layer with the brighter layer at the top is more apparent.

To identify the nature of the two sublayers in the multilayer structure, EDS elemental mappings were acquired in the same areas shown in Fig. 2. Here, the EDS result of the irradiated region with

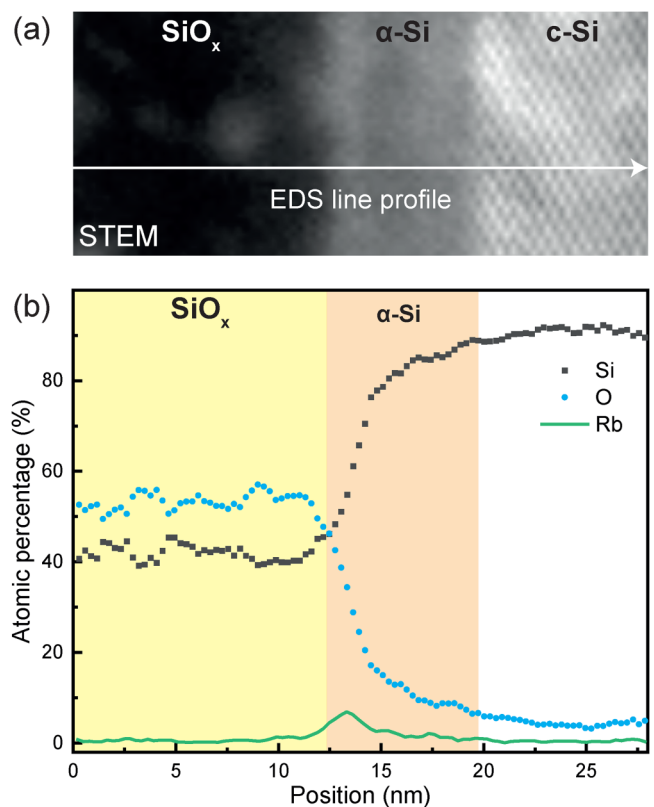


FIG. 4. (a) STEM-HAADF image of the top part of an irradiation Si sample at a dose of 3×10^{17} ions/cm²; (b) quantitative elemental composition profile across the stack by EDS mapping. Dark points (black) represent Si, light points (blue) for O, and the solid curve (green) is for Rb.

28 June 2023 08:50:39

the ion dose of 2×10^{16} ions/cm² is shown in Fig. 3 as an example. In the HAADF-STEM mode, the image brightness scales approximately with the atomic number squared. It can be seen that now the top layer is darker compared to the lower layer as shown in Fig. 3(a), which indicates a small difference in elemental composition between the two layers. Figure 3(b) shows the EDS mapping of four elements in the area shown in Fig. 3(a). Silicon can be detected in the top and lower layers, while oxygen is found in the top layer only. It should be noted that rubidium is observed in the lower layer and also seems to be present in the Pt deposition layer, but the latter can be explained by partly overlapping peaks in the EDS spectrum, see Fig. 3(c). For the Rb mapping, the K-lines have been used, as the Rb-L peak (1.69 keV)—although higher in intensity than the Rb K-lines—has a strong overlap with the high-intensity Si K α peak (1.74 keV) from the substrate, making an accurate determination of the Rb content impossible. As an alternative, the Rb K peaks can be used. Figure 3(c) displays EDS spectra in the energy range of 12–16 keV, corresponding with the four stacked layers shown in Fig. 3(a). Two obvious peaks can be seen in the green curve (corresponding to the lower layer), which represent the Rb-K α (13.37 keV) and K β peaks (14.96 keV), respectively. Concerning the red curve (Pt deposition layer), there are also two peaks near 13 keV, identified as Pt-L γ peaks. There cannot be any Rb in the Pt dep layer, since Pt was deposited in the Dual-beam FIB system after the Rb irradiation step. Thus, the overlap between the Pt-L γ peaks and Rb-K α peak indeed leads to a wrong assignment of the rubidium distribution in the Pt layer. From the EDS mapping results and spectrum analysis, the top layer of the sample

itself only contains silicon and oxygen without any rubidium, while silicon and rubidium are detected in the lower layer.

To avoid such erroneous quantification of Rb and Pt, the testing area is chosen to include part of the top layer, lower layer, and crystal silicon (c-Si) substrate without Pt capping, as shown in Fig. 4(a). A quantitative elemental profile, extracted from the EDS mapping of the region shown in Fig. 4(a) is presented in Fig. 4(b). It is observed that in the topmost layer [the left region in Fig. 4(a)], there is almost no Rb, but about 55% O with around 40% Si. It is more like an oxidation layer after damage and can be called the “SiO_x” layer. The middle region in Fig. 4(a), it has around 90% Si and low content of O. Thus, this layer can be seen as the α -Si layer. An Rb peak is shown near the interface between the SiO_x layer and α -Si layer with a peak value of 7% in atomic percentage. Beyond that, an undamaged crystalline Si layer is apparent.

Ion staining is another key factor to characterize ion irradiation damage. Here, the Rb concentration profiles for a series of ion doses are presented in Fig. 5(a), as well as the SRIM (Stopping and Range of Ions in Matter) simulation results [shown in Fig. 5(b)]. The zero point position in the figures corresponds to the Pt/Si interface. In general, the Rb peak shifts from the near-surface region to deeper sites as the ion dose increases. At the lowest ion dose of 2×10^{15} ions/cm² (green dashed curve), the Rb distribution is mainly concentrated in the range of 7–18 nm from the interface (25%–75% of peak value). The curve is similar to the SRIM simulation results, where the predicted Rb stopping range is 6–20 nm. For a higher ion dose irradiation of 2×10^{16} ions/cm², the Rb curve keeps a similar same shape but the peak shifts to around 15 nm

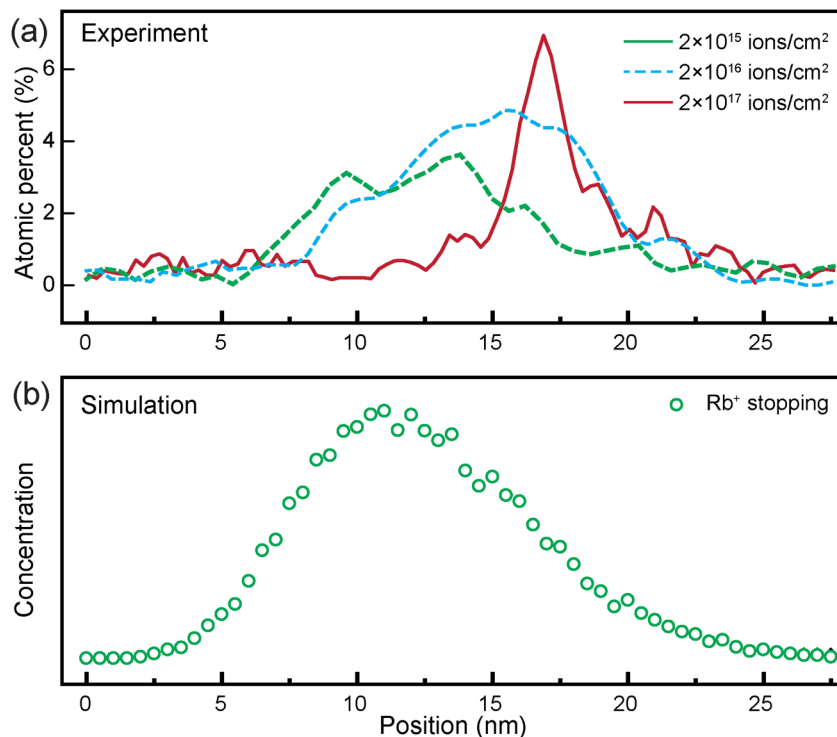


FIG. 5. (a) Experimental result of Rb⁺ distribution at the dose of 2×10^{15} ions/cm² (thick dashed line) (green), 2×10^{16} ions/cm² (thin dashed line) (blue), and 2×10^{17} ions/cm² (solid line) (red). (b) SRIM simulation results of the distributions of Rb⁺ ion stopping sites.

28 June 2023 08:50:39

from the interface. At the highest ion dose irradiation of 2×10^{17} ions/cm², the distribution has a sharper peak curve compared to the low ion dose irradiation. The peak shifts from 15 to about 17 nm from the interface, and the peak value of the Rb content is about 7%, which can be seen as the stationary Rb⁺ staining level in Si. The staining level is much lower compared to that of Ga in Si irradiated by Ga⁺ ions as described in Sec. I. Similar work was reported by Drezner *et al.*¹⁸ in which the Cs staining level is measured to be 11.5% in Si. They suggest the possible explanation for the change in the shape of the distribution could be a high self-sputtering rate of implanted ions by new incident ions.

In schematic form, Fig. 6 poses a sequence of steps resulting from Rb⁺ irradiation of an Si substrate to explain the observations. At the start of the ion irradiation, the Rb⁺ ions penetrate the Si substrate, collide with silicon atoms, and generate damage leading to amorphization. Figure 6(a) shows that at low ion dose, Rb⁺ ions sputter Si atoms, concentrate in the incident volume, and part of them can reach a deep site from the surface. As predicted by SRIM, the ion range of Rb⁺ is 12.9 nm, but a small fraction of the Rb⁺ ions will reach 20 nm depth from the surface in Si. With the increase of impinging Rb⁺ ions, as shown in

Fig. 6(b), there is more Rb concentrated in the near-surface region of the Si substrate, part of which is then sputtered and thus removed by the incident ions, while another part is propelled from the near-surface area to a deeper site. Due to the volatility of Rb, it evaporates from the surface after the irradiation [Fig. 6(c)]. It is known that Rb has a high diffusion in crystalline Si substrate.²⁸ In addition, the Rb trapped near the surface can also get enough thermal energy to overcome a surface barrier potential during repeated scanning of the irradiating ion beam.²⁹ A high dose furthermore leads to a more porous structure of the Si substrate, which enhances Rb evaporation in deeper regions. This leads to the shift of Rb concentration observed in Fig. 5. The formation of the SiO_x layer is then mainly caused by the introduction of oxygen to the irradiated area as shown in Fig. 6(d). One possibility is the presence of residual oxygen gas or water in the FIB vacuum chamber during milling, but more likely is that it results from air exposure during the sample transportation from the Rb FIB to the Dual-beam FIB. Such an oxidation process might occur preferably in the porous Si regions and form a barrier layer to prevent outer oxygen penetration and rubidium evaporation. The precise reason for the oxidation and the role of

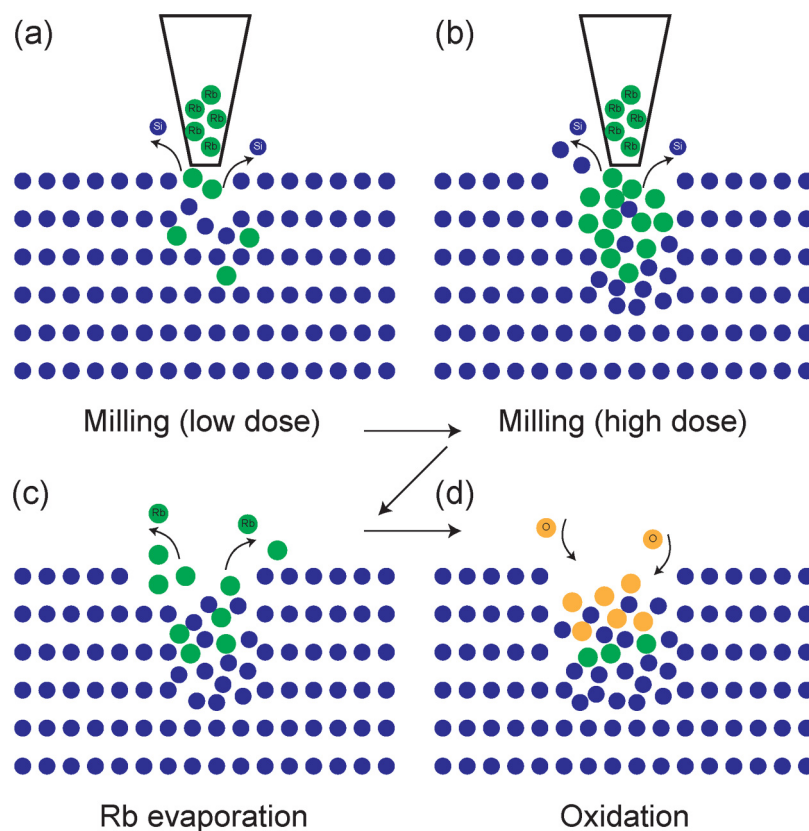


FIG. 6. Schematic progress of Rb⁺ ion damage formation on the Si substrate. (a) A Si substrate is milled under the Rb⁺ ion beam at a low ion dose; (b) the same substrate is milled under the Rb⁺ ion dose at a high ion dose; (c) Rb evaporates from the surface after the milling process; (d) simultaneously, some oxygen are introduced into the irradiated area. Dark dots (blue) represent Si, dark gray (green) is for Rb and in subfigure (d) light gray (orange) represents O.

28 June 2023 08:50:39

Rb in the process could be further investigated through control experiments involving, e.g., flushing the system with hydrogen gas to terminate the reaction or applying an HF dip and analyzing samples milled with Ga under comparable conditions to check for the prevalence of oxygen layers.

It should be noted that our studies are focused on the 0° incidence of Rb⁺ ion beams on Si substrates with circuit edit as an application in mind. The majority of FIB nanomachining applications are TEM sample preparation and cross sections, which is concerned with ion staining and lateral damage under irradiation at glancing angle. From SRIM simulations, the penetration depth of Rb⁺ ions at a glancing angle (> 80°) would be around 4 nm at the beam energy of 8.5 keV. It may then be possible to have lower ion staining at sidewalls after cross sectioning due to the smaller lateral ion range and the volatility of Rb. Future study could, therefore, be focused on the beam damage evaluation at the glancing angle irradiation as a further test of the suitability of Rb CAIS-FIB system.

IV. CONCLUSIONS

A series of Rb⁺ irradiation experiments at 8.5 keV beam energy under normal incidence has shown a 22.2(±0.3) nm thick damage layer in silicon substrates. A multilayer damage structure is observed consisting of an oxidation layer and an amorphous silicon layer. With increasing of ion dose, the thickness of the oxidation layer also increases, from 3.3(±0.1) nm (3×10^{17} ions/cm²) to 4.4 (±0.1) nm and 5.1(±0.1) nm, and, finally, to 16.2(±0.2) nm (3×10^{17} ions/cm²). The measured Rb⁺ staining level in Si is 7(±1)% in atomic weight. This damage layer thickness, and ion staining level is comparable to what was observed for Cs⁺ irradiation¹⁸ under somewhat similar circumstances.

ACKNOWLEDGMENTS

This work is part of the project Next-Generation Focused Ion Beam (No. 16178) of the research programme Applied and Engineering Sciences (TTW), which is (partly) financed by the Dutch Research Council (NWO). The authors are (partly) members of the FIT4NANO COST Action CA19140. Solliance and the Dutch province of Noord-Brabant are acknowledged for funding the STEM facility. The authors thank helpful discussions with Greg Schwind, Chad Rue, Yuval Greenzweig, and Peter Graat.

AUTHOR DECLARATIONS

Conflict of Interest

The authors have no conflicts to disclose.

Author Contributions

S. Xu: Data curation (equal); Formal analysis (equal); Investigation (equal); Writing – original draft (equal); Writing – review & editing (equal). **Y. Li:** Investigation (supporting); Writing – review & editing (equal). **M. A. Verheijen:** Formal analysis (equal); Writing – review & editing (equal). **E. R. Kieft:** Formal analysis (equal); Writing – review & editing (supporting). **E. J. D.**

Vredendregt: Supervision (equal); Writing – review & editing (equal).

DATA AVAILABILITY

The data that support the findings of this study are available from the corresponding author upon reasonable request.

REFERENCES

- ¹N. Bassim, K. Scott, and L. A. Giannuzzi, *MRS Bull.* **39**, 317 (2014).
- ²P. R. Munroe, *Mater. Charact.* **60**, 2 (2009).
- ³P. Li *et al.*, *Nanoscale* **13**, 1529 (2021).
- ⁴J. Li, T. Malis, and S. Dionne, *Mater. Charact.* **57**, 64 (2006).
- ⁵J. Huang, M. Loeffler, U. Muehle, W. Moeller, J. Mulders, L. T. Kwakman, W. Van Dorp, and E. Zschech, *Ultramicroscopy* **184**, 52 (2018).
- ⁶Y. Greenzweig, Y. Drezner, S. Tan, R. H. Livengood, and A. Raveh, *Microelectron. Eng.* **155**, 19 (2016).
- ⁷S. Rubanov and P. Munroe, *J. Microsc.* **214**, 213 (2004).
- ⁸Y. Xiao, F. Fang, Z. Xu, W. Wu, and X. Shen, *Nucl. Instrum. Methods Phys. Res. B* **307**, 253 (2013).
- ⁹J. Morgan, J. Notte, R. Hill, and B. Ward, *Microsc. Today* **14**, 24 (2006).
- ¹⁰M. E. Schmidt, T. Iwasaki, M. Muruganathan, M. Haque, H. Van Ngoc, S. Ogawa, and H. Mizuta, *ACS Appl. Mater. Interfaces* **10**, 10362 (2018).
- ¹¹D. Emmrich, A. Beyer, A. Nadzeyka, S. Bauerdick, J. Meyer, J. Kotakoski, and A. Götzhäuser, *Appl. Phys. Lett.* **108**, 163103 (2016).
- ¹²R. Li, R. Zhu, S. Chen, C. He, M. Li, J. Zhang, P. Gao, Z. Liao, and J. Xu, *J. Vac. Sci. Technol. B* **37**, 031804 (2019).
- ¹³R. Livengood, S. Tan, Y. Greenzweig, J. Notte, and S. McVey, *J. Vac. Sci. Technol. B* **27**, 3244 (2009).
- ¹⁴S. Hang, Z. Mektadir, and H. Mizuta, *Carbon* **72**, 233 (2014).
- ¹⁵J. J. McClelland, A. V. Steele, B. Knuffman, K. A. Twedt, A. Schwarzkopf, and T. M. Wilson, *Appl. Phys. Rev.* **3**, 011302 (2016).
- ¹⁶B. Knuffman, A. V. Steele, and J. J. McClelland, *J. Appl. Phys.* **114**, 044303 (2013).
- ¹⁷See <https://www.zerok.com> (accessed September 9, 2022).
- ¹⁸Y. Drezner, Y. Greenzweig, and A. Raveh, *J. Vac. Sci. Technol. B* **34**, 061203 (2016).
- ¹⁹S. Wouters, “A compact, ultracold atomic beam source for use in a focused ion beam,” Ph.D. thesis (Eindhoven University of Technology, 2016), available at https://pure.tue.nl/ws/portalfiles/portal/48404154/20161214_Wouters.pdf.
- ²⁰G. Ten Haaf, “Ultracold Rb focused ion beam,” Ph.D. thesis (Eindhoven University of Technology, 2017). See https://pure.tue.nl/ws/files/81094890/20171121_ten_Haaf.pdf.
- ²¹G. ten Haaf, S. Wouters, D. Nijhof, P. Mutsaers, and E. Vredendregt, *Ultramicroscopy* **190**, 12 (2018).
- ²²S. Xu, Y. Li, and E. Vredendregt, *J. Vac. Sci. Technol. B* **40**, 042801 (2022).
- ²³Y. Li, S. Xu, M. Sezen, F. B. Misirlioglu, and E. Vredendregt, *J. Vac. Sci. Technol. B* **41**, 042803 (2023).
- ²⁴G. ten Haaf, S. H. W. Wouters, S. B. van der Geer, E. J. D. Vredendregt, and P. H. A. Mutsaers, *J. Appl. Phys.* **116**, 244301 (2014).
- ²⁵G. ten Haaf, T. C. H. de Raadt, G. P. Offermans, J. F. M. van Rens, P. H. A. Mutsaers, E. J. D. Vredendregt, and S. H. W. Wouters, *Phys. Rev. Appl.* **7**, 054013 (2017).
- ²⁶G. ten Haaf, S. H. W. Wouters, P. H. A. Mutsaers, and E. J. D. Vredendregt, *Phys. Rev. A* **96**, 053412 (2017).
- ²⁷J. Mayer, L. A. Giannuzzi, T. Kamino, and J. Michael, *MRS Bull.* **32**, 400 (2007).
- ²⁸J. McCaldin and A. Widmer, *Proc. IEEE* **52**, 301 (1964).
- ²⁹S. Atutov, F. Benimetskii, and A. Makarov, *Optoelectron., Instrum. Data Process.* **53**, 278 (2017).
- ³⁰See supplementary material online for the corresponding low-magnification TEM images.

28 June 2023 08:50:39